

Maximum Likelihood Analysis of Clusters of Ultra-High Energy Cosmic Rays

Günter Sigl, Martin Lemoine, and Angela V. Olinto

Department of Astronomy & Astrophysics

Enrico Fermi Institute, The University of Chicago, Chicago, IL 60637-1433

(September 28, 2018)

We present a numerical code designed to conduct a likelihood analysis for clusters of nucleons above 10^{19} eV originating from discrete astrophysical sources such as powerful radio galaxies, γ -ray bursts or topological defects. The code simulates the propagation of nucleons in a large-scale magnetic field and constructs the likelihood of a given observed event cluster as a function of the average time delay due to deflection in the magnetic field, the source activity time scale, the total fluence of the source, and the power law index of the particle injection spectrum. Other parameters such as the coherence length and the power spectrum of the magnetic field are also considered. We apply it to the three pairs of events above 4×10^{19} eV recently reported by the Akeno Giant Air Shower Array (AGASA) experiment, assuming that these pairs were caused by nucleon primaries which originated from a common source. Although current data are too sparse to fully constrain each of the parameters considered, and/or to discriminate models of the origin of ultra-high energy cosmic rays, several tendencies are indicated. If the clustering suggested by AGASA is real, next generation experiments with their increased exposure should detect more than ~ 10 particles per source over a few years and our method will put strong constraints on both the large-scale magnetic field parameters and the nature of these sources.

PACS numbers: 98.70.Sa, 98.62.En

I. INTRODUCTION

Despite more than 30 years of experiments on ultra-high energy cosmic rays (UHECRs), i.e., air showers with primary energy $E \gtrsim 1$ EeV ($= 10^{18}$ EeV), the origin of these particles remains unknown. The most distinctive feature of the energy spectrum of UHECRs is undoubtedly the “ankle”, at $E \simeq 10^{18.5}$ eV [1,2]. The cosmic ray spectrum is steep up to the ankle, corresponding to a differential power law index of $\simeq -3.1$, and flattens beyond, with an index $\simeq -2.7$. Data from the Fly’s Eye experiment also suggest that the chemical composition is dominated by heavy nuclei, presumably iron, up to the ankle, and by protons beyond [1]. Hence, the ankle might mark a transition from galactic to extra-galactic origin [1,2]. This idea is supported by the observed isotropy of cosmic rays for $E \gtrsim 4 \times 10^{19}$ eV [3], together with the fact that charged particles with $E \gtrsim 10^{19}$ eV have too large a gyro-radius in the galactic magnetic field to be confined. However, in analogy to the γ -ray burst (GRB) phenomenon, an origin of UHECRs in an extended galactic halo cannot be excluded thus far.

If UHECRs with $E \gtrsim 10^{18.5}$ eV are indeed protons of extra-galactic origin, one would expect to detect the so-called Greisen-Zatsepin-Kuzmin cutoff [4] (hereafter GZK) due to photopion production on the cosmic microwave background (CMB) by nucleons of energy $E \gtrsim$

70 EeV. The presence of this cutoff has been suggested by various experiments, although the energy spectrum around $E \simeq 100$ EeV is yet to be agreed upon. Nonetheless, the combined data of the Haverah Park, Yakutsk, Fly’s Eye, and AGASA experiments give 7 detected events above 100 EeV, for 22 expected from extrapolation of lower energy data, which provides a strong hint toward the presence of a cutoff [2]. Finally, a 2σ detection of this GZK cutoff has been recently claimed by the AGASA experiment from the combined data 1991-1996 [5].

Photopion production on the CMB limits the range of nucleons above 100 EeV to about 30 Mpc, whereas heavy nuclei are photodisintegrated on an even shorter distance scale [6]. In this frame, the detection of UHECRs with $E \gtrsim 100$ EeV [7,1,8,9,2] has triggered considerable discussion in the literature on the nature and origin of these particles [10–12]. Indeed, even the most powerful astrophysical objects such as radio galaxies, quasars, and active galactic nuclei are barely able to accelerate charged particles to such energies [13]. Moreover, there is no obvious optical or radio counterpart to these UHECR events at a distance less than a few hundred Mpc. For the highest energy event observed, $E \simeq 3 \times 10^{20}$ eV [7], the quasar 3C 147 is the best candidate as far as energetics is concerned; however, it lies ~ 1 Gpc away, and if the primary were a proton, its injection energy would have to be

$E > 10^{22}$ eV. A similar problem arises for the less likely option of a γ -ray primary [12], whereas neutrino primaries in general imply too large a flux because of their small interaction probability in the atmosphere [14].

Currently, there are three main classes of models for the origin of UHECRs. The most conventional one assumes first order Fermi acceleration of protons at astrophysical magnetized shocks (see, e.g., Ref. [15]). This mechanism is usually associated with prominent astrophysical objects such Fanaroff-Riley Class II radio galaxies, either in the hot spots or in the lobes [16] and could accelerate protons up to $E \sim 10^{21}$ eV.

It has also been suggested that UHECRs could be associated with cosmological γ -ray bursts (GRBs) [17–20]. This is mainly motivated by the fact that the required average rate of energy release in γ -rays is comparable to the one in UHECRs above 10 EeV turn out to be comparable. Protons could be accelerated beyond 100 EeV within the relativistic shocks associated with fireball models of cosmological GRBs [21]. Since the rate of cosmological GRBs within the field of view of the cosmic ray experiments which detected events above 100 EeV is about 1 per 50 yr, a dispersion in UHECR arrival times of at least 50 yr is necessary to reconcile the observed UHECR and GRB rates. Such a dispersion could be caused by the time delay of protons acquired through their deflection in large-scale magnetic fields (LSMF) [17,18]. However, this requirement could be circumvented in a model where UHECRs are produced in a galactic halo population of GRBs [22].

Finally, so-called “top-down” models constitute another class of scenario. There, particles are created at extremely high energy in the first place by the decay of some supermassive elementary “X” particle associated with new physics near the grand unification scale [23]. Such theories predict phase transitions in the early universe that are expected to create topological defects such as cosmic strings, domain walls or magnetic monopoles. Although such defects are topologically stable and would be present today, they could release X particles due to physical processes such as collapse or annihilation. Among the decay products of the X particle are jets of $10^4 - 10^5$ hadrons most of which are in the form of pions that subsequently decay into γ -rays, electrons, and neutrinos. Only a few percent of the hadrons are expected to be nucleons [24]. Thus, typical features of these scenarios are the predominant release of γ -rays and neutrinos, and spectra that are considerably harder than in the case of shock acceleration. For more details about these models, see, e.g., Ref. [25].

Recently, a possible correlation of a subset of events above 40 EeV among each other and with the supergalactic plane was reported by the AGASA experiment [3]. Among 20 events with energy above 50 EeV, two pairs of events with an angular separation of less than 2.5° were observed within 10° of the supergalactic plane at an angular resolution of $\simeq 1.6^\circ$. The probability for that to happen by chance for an isotropic, unclustered distribu-

tion is $\simeq 4 \times 10^{-4}$. A third pair was observed among 36 showers above 40 EeV, with a chance probability of about 6×10^{-3} . Although the muon content of the showers suggests that the primaries are protons in each case, γ -rays cannot be excluded [3]; in the following, however, we will assume that the primaries are protons.

This suggests that the events within one pair have been emitted by a single discrete source possibly associated with the large-scale structure of the galaxies. The deflection of a charged particle in a magnetic field is inversely proportional to its energy E . Therefore, the fact that the lower energy event in the pair with the greatest energy difference (see Table I) arrived later might hint to the pair’s origin in a burst, i.e., on a time scale $\lesssim 1$ yr. The time delay would then be dominated by magnetic deflection of the lower energy particle. Even the two other pairs observed by AGASA, in which the higher energy particle arrived later, could have originated in a burst. Since the average time delay due to magnetic deflection, τ_E , scales as $\tau_E \propto E^{-2}$, the dispersion in time delay is bounded from below by twice the energy resolution, $\Delta\tau/\tau \approx 0.6$, and could be as large as ~ 2 [26]. Furthermore, the distance to the source cannot be much larger than $\simeq 100$ Mpc, if the higher energy primary was either a nucleon, a nucleus, or a γ -ray, since its energy was observed to be $\gtrsim 75$ EeV in all three pairs.

Pair #	Energy [EeV]	date	b^{SG}	b^{G}
1	210	93/12/03	0.4	-41.1
	51	95/10/29	1.1	-42.3
2	78	95/01/26	0.5	56.9
	55	92/08/01	2.0	55.3
3	110	94/07/06	57.3	18.6
	43	91/04/20	57.8	21.2

TABLE I. Properties of the pairs observed by AGASA. b^{SG} and b^{G} are the supergalactic and the galactic latitude, respectively.

Possible explanations of these observations rest not only on the model of UHECR origin but also on the largely unknown features of the LSMF (for a review see, e.g., Ref. [27]). Here, we call LSMF both extra-galactic fields with strengths $10^{-12} \text{ G} \lesssim B_{\text{rms}} \lesssim 10^{-9} \text{ G}$ as well as fields in the halo of our Galaxy with $10^{-8} \text{ G} \lesssim B_H \lesssim 10^{-6} \text{ G}$. In the present paper, we show how the distribution of arrival times and energies of clusters of UHECR events originating from the same astrophysical source such as the ones suggested by AGASA can be used to constrain both the nature of the source and the structure of the LSMF. We restrict ourselves to nucleons and perform Monte Carlo simulations of their propagation through the LSMF. Then we construct the likelihood as a function of several parameters characterizing the LSMF and the source of the pairs observed by AGASA. We describe our Monte-Carlo simulations and the likelihood analysis in Sect. 2. In Sect. 3, we discuss our findings

and their implications for the structure of the LSMF and for the models of UHECR origin. Sect. 4 concludes with a discussion of the future prospects of the method presented in this paper.

II. NUMERICAL SIMULATIONS

A. The Monte-Carlo code

Previous works have focused on various aspects of non-diffusive, nearly straight-line propagation of extremely high energy nucleons in LSMF. In Ref. [26] the diffusion problem was studied, in the limits $D\theta_E \ll l_c$ and $D\theta_E \gg l_c$, where D is the distance to the source, θ_E is the r.m.s. deflection angle, which is a function of energy E , and l_c is the coherence length of the magnetic field. However, these authors did not consider pion production, and their results are only valid for energies $E \lesssim 50$ EeV. In Refs. [28–30] propagation codes that follow multiple species were constructed, taking all types of interactions into account, although neglecting any scattering on the magnetic field; thus these calculations cannot treat the time delay of UHECRs. Finally, the authors of Ref. [31] carried out tri-dimensional Monte-Carlo simulations, including pion production effects and scattering off magnetic field inhomogeneities. In their work, pion production is treated as a continuous energy loss process and its stochastic nature is neglected. The magnetic field configuration is simplified to an assembly of coexistent bubbles of randomly aligned dipole fields, with a diameter given by the coherence length of the field.

To properly calculate the desired likelihood, one has to consider both pion production and deflection on cosmic magnetic fields. Thus we devised a Monte Carlo code, which improves on the treatment in Ref. [31] on the points discussed in the following.

Pion production is treated in the appropriate stochastic way, as described in Ref. [30]; namely, the occurrence, and the nature of the secondary and its energy are randomly drawn from the relevant probability distributions. Since the fractional energy loss of a proton in a pair production event is about the ratio of the electron to the proton mass, pair production can be included into the equations of motion as a continuous energy loss term, for which we used the expressions in Ref. [32].

The LSMF are described as gaussian random fields, with zero ensemble average, and a power spectrum given by $\langle B^2(k) \rangle \propto k^{n_B}$ for $k < 2\pi/l_c$, and $\langle B^2(k) \rangle = 0$ otherwise. The cutoff, l_c , characterizes the coherence length of the field. The phase and direction of the field are drawn from uniform random distributions. Note that for the time delay calculation only the field component perpendicular to the line-of-sight contributes. This model can thus be characterized by three parameters: the power-law index n_B , the coherence scale l_c , and the r.m.s. field strength, given by $B_{\text{rms}}^2 \equiv V/(2\pi)^3 \int d^3\mathbf{k} B^2(\mathbf{k})$.

The precise structure of the LSMF is unknown, but estimates can be made for different cases. Extra-galactic fields with cosmological origins have $n_B \simeq 0$ and $l_c \simeq 1$ Mpc [33]. For halo fields to cause notable delays, $l_c \gtrsim 1$ kpc. Note that for these large coherence lengths the dynamical range probed by UHECRs is not very sensitive to n_B .

In addition to the LSMF defined above, there are localized fields associated with galaxies, clusters of galaxies, and the large scale galaxy distribution. The small filling factors of galaxies, $f_G \sim 10^{-4}$, and clusters, $f_C \sim 10^{-6}$, justify neglecting their effect. If galactic and cluster outflows are efficient polluters of the extra-galactic medium, their effect can be modeled by the extra-galactic field considered above. The filling factor for such pollution fields was estimated to $\simeq 10\%$ for a field strength considerably smaller than $\sim \mu\text{G}$ [34].

Fields associated with the galaxies large scale structure may significantly affect UHECR propagation. In fact, the arrival directions of two of the three pairs observed by AGASA (see Table I) are very close to the supergalactic plane; reinforcing the claim for a supergalactic plane correlation of UHECRs [35]. As was subsequently pointed out in Ref. [36], this correlation seems to be even stronger than expected if the origin of UHECRs were associated with the large-scale galaxy structure, as the supergalactic plane alone is not a good approximation of this latter. As a solution, it has been suggested, in Refs. [37,38], that the possible existence of strong fields, with strengths up to μG and coherence lengths in the Mpc range, aligned along the large-scale structure, could produce a focusing effect of UHECRs along the sheets and filaments of galaxies. However, since UHECR propagation would take place mainly along the strong coherent field component, effects on the time delay would be much smaller than those induced by an incoherent field of comparable strength. Within a first approximation, therefore, we can neglect such coherent strong field components in our present analysis, which rests primarily on the time delay effect. In other words, our analysis is sensitive mainly to the weaker random field components that are not aligned with the large-scale structure sheets and filaments.

We also neglect the influence of the magnetic field in the disk of our Galaxy. Denoting its typical strength by B_d and its scale by l_d , the deflection angle θ_E for a proton at energy E arriving from above or below the galactic disk is

$$\theta_E \simeq 5.5^\circ \left(\frac{E}{10 \text{ EeV}} \right)^{-1} \left(\frac{l_d}{1 \text{ kpc}} \right) \left(\frac{B_d}{10^{-6} \text{ G}} \right) \sin \theta, \quad (1)$$

where θ is the angle between the field polarization and the arrival direction of the particle. The corresponding time delay, $\tau_E \simeq \theta_E^2 l_d / 2$, is small compared to the measurement period of a few years and can be neglected for $E \gtrsim 10$ EeV in our analysis, if $l_g \lesssim 100$ pc and $B_d \lesssim 10^{-6}$ G, which are typical values for the disk field.

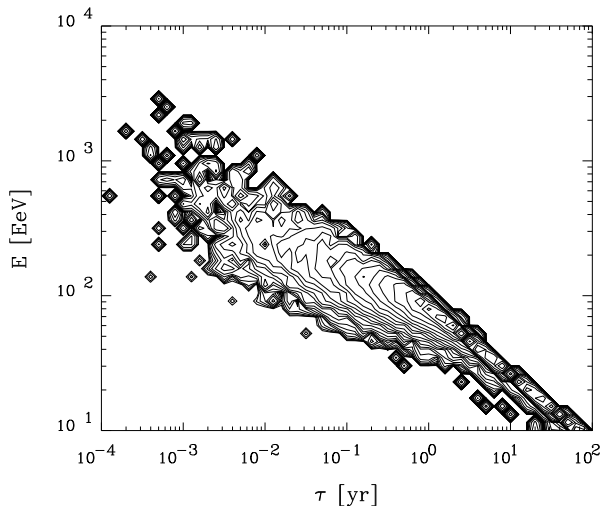


FIG. 1. Contour plot for a distribution of events originating from a bursting source, as projected in the time-energy plane. The corresponding parameters are $D = 30$ Mpc, $B_{\text{rms}} = 10^{-11}$ G, $n_B = 0$, $l_c = 1$ Mpc; the differential index of the energy injection spectrum is -2.0 . Deviations from the mean correlation $\tau_E \propto E^{-2}$, for $E \geq 70$ EeV, reflect pion production on the CMB. In order to show the statistics at high energies, 40 contours with logarithmic decrements of 0.15 in the logarithm to base 10, are shown.

We also remark that none of the AGASA pair arrival directions lie close to the galactic plane (see Table I). We will assume that the actual time delay is dominated either by the extra-galactic magnetic field or by an extended galactic halo field. Under this assumption, observed time dispersions contain information only about the extra-galactic magnetic field or the galactic halo field [39].

Once the configuration of the LSMF is set, via Fast Fourier Transform methods, on a lattice with inter-cell separation $l_c/2$ and typical size 64^3 or 128^3 , a sample of nucleons is propagated over a distance D in a randomly chosen direction. The integration is achieved via the usual fourth order adaptive step size Runge-Kutta integration (see, e.g., Ref. [40]). At each time step, the nucleons are subjected to deflection by the local magnetic field, are tested against pion production and β decay if the nucleon is a neutron, and pair production energy loss is taken into account.

Angle-time-energy images of a discrete source at a fixed location depend on the specific LSMF structure which the nucleons encounter during their propagation [39]. In principle, one has to simulate a discrete source by emitting particles isotropically from the origin, and keeping those particles that arrive on the sphere of radius D within a solid angle segment small compared to the squared r.m.s. deflection angle. This is crucial in the limit of small deflection, $D\theta_E \ll l_c$; this limit is also the most probable for typical extra-galactic magnetic fields (see Eq. (2) below, see also Ref. [39]). In the opposite

limit, $D\theta_E \gg l_c$, where nucleons following different paths experience different magnetic field configurations, it is sufficient to send the particles isotropically, and average over all events independently of their arrival location. The effect of these two limits on the resulting angle-time-energy image of the source was pointed out in Ref. [26]. In the limit of small deflection, the scatter around the mean correlations, $\tau_E \propto E^{-2}$ and $\theta_E \propto E^{-1}$, is expected to be negligible below the photopion production threshold, with $\Delta E/E \sim 1\%$. In the opposite limit, $D\theta_E \gg l_c$, the stochastic deflections of different nucleons off different magnetic inhomogeneities imply a significant scatter, with $\Delta E/E \sim 30\%$. We confirmed that our code yields distributions in energy and time that are consistent with the analytical expression given in Ref. [26] for this case, below the GZK cutoff.

In order to simulate the small deflection limit, one has to restrain oneself to defining a receiving cone angle smaller than the r.m.s. deflection angle, and to selecting an emission cone angle not much larger than the receiving angle. This will in general introduce a bias in the simulated energy spectrum, notably because the r.m.s. deflection angle is a function of energy. In order to correct for this bias, we renormalize the time-integrated flux at a given energy to the corresponding flux for vanishing magnetic fields. This is appropriate in our case, where delay times are much smaller than energy loss distances, i.e., where the magnetic field has no influence on the time-integrated energy spectrum. Fig. 1 shows an example for the resulting distributions of arriving particles in time and energy for a bursting source, in the small deflection limit. For a more general discussion of the angle-time-energy images of UHECR sources, see Ref. [39].

B. Likelihood

We wish to evaluate the likelihood of the observations of the three AGASA pairs as a function of the different parameters characterizing the origin of UHECRs and the nature of their energy spectrum, as well as those characterizing the LSMF. We thus consider the following. We assume that the source emits UHECRs on the time scale T_S ; for a burst, $T_S \ll 1$ yr. We group together the distance to the source, D , the coherence length l_c , the r.m.s. magnetic field strength B_{rms} , and the magnetic power spectrum index n_B , in the average time delay τ_E ; this latter is calculated from the expressions given in Ref. [26], as:

$$\tau_E \simeq 0.22 \left(\frac{3 + n_B}{2 + n_B} \right) \left(\frac{D}{30 \text{ Mpc}} \right)^2 \left(\frac{E}{100 \text{ EeV}} \right)^{-2} \times \left(\frac{B_{\text{rms}}}{10^{-11} \text{ G}} \right)^2 \left(\frac{l_c}{1 \text{ Mpc}} \right) \text{ yr.} \quad (2)$$

This follows from a random walk argument, and is, strictly speaking, a good approximation only below the

pion production threshold and in the large deflection limit, $D\theta_E \gg l_c$. We also consider the distance D as a separate parameter, as it governs the amplitude of pion production, hence the propagated UHECR energy spectrum.

For the total energy output of the source in UHECRs above an energy E , we assume a power law, $\mathcal{E}(> E) \propto E^{-\gamma+2}$, and consider three different representative values for the index γ , namely $\gamma = 1.5, 2.0$, and 2.5 . A hard spectrum with $\gamma = 1.5$ is typical for defect models [23,25], whereas softer spectra with $\gamma \gtrsim 2.0$ are typical for acceleration at astrophysical shocks [15]. With respect to observations, it is more convenient to characterize the total energy output with the total number of particles $N(E_0)$, that would be detected by the experiment with an energy $E \geq E_0$, over an infinite integration time,

$$N(E_0) \simeq 2 \times 10^2 f_d \left(\frac{A}{100 \text{ km}^2} \right) \left(\frac{D}{30 \text{ Mpc}} \right)^{-2} \quad (3)$$

$$\times f_s(E_0) \left(\frac{E_0}{10^{1.5} \text{ EeV}} \right)^{-1} \left(\frac{\mathcal{E}(> E_0)}{10^{51} \text{ erg}} \right).$$

Here, f_d denotes the experimental duty cycle with respect to having the source in the field of view, A is the effective detection area of the experiment under consideration, and $f_s(E_0)$ is a dimensionless factor of order unity that depends weakly on the energy injection spectrum cutoff. Eq. (3) is valid below the pion production threshold and in the following we take $E_0 = 10^{1.5} \text{ EeV}$ which is the energy above which the 3 AGASA pairs have been observed, within the energy resolution. We consider values for $N(10^{1.5} \text{ EeV})$ between 1 and 4000 particles, which is a typical range to be expected for the fiducial values in Eq. (3).

The main parameters defining the likelihood are therefore T_S , $\tau_{100} \equiv \tau_{E=100 \text{ EeV}}$, D , γ , and $N_0 \equiv N(E_0 = 10^{1.5} \text{ EeV})$; secondary parameters are l_c and n_B . The likelihood is calculated in the standard way for each observed event cluster denoted by i_P , using Poisson statistics,

$$\mathcal{L}(\tau_{100}, T_S, D, \gamma, N_0, i_P) \equiv \prod_{j=1, N} e^{-\rho_j} \frac{\rho_j^{n(j, i_P)}}{n(j, i_P)!}, \quad (4)$$

where ρ_j is the predicted number of events in cell j , and $n(j, i_P)$ is the number of observed events (either 0 or 1 in our case) in cell j for the observed event cluster i_P . Each cell is defined by a time coordinate and an energy. We binned the time-energy histogram to logarithmic energy bins of size 0.1 in the logarithm to base 10, and to 0.1 yr in linear time bins (we are limited to 0.1 yr time resolution because of memory size). The product in the formula above extends over all energy bins (from $10^{1.5} \text{ EeV}$ to 10^4 EeV) and over all time bins that are comprised within an observational time window of length T_{obs} ; we took $T_{\text{obs}} \simeq 5 \text{ yr}$, as AGASA started operating in 1990, and the latest data reported date back to the end of October 1995.

The likelihood as given above has already been marginalized over two auxiliary parameters: a zero-point in time t_0 , which defines the position of the observational time window on the time delay histogram of the UHECRs, and the path that the particle followed through the magnetic field. The first marginalization over t_0 is carried out by drawing t_0 at random a large number of times from a uniform distribution, calculating the likelihood, and averaging the resulting likelihood over t_0 with equal weights. The second marginalization is carried out in a similar spirit, i.e., by separately calculating likelihoods for different realizations of the LSMF between the source and the observer and averaging them with equal weights.

The likelihood defined in Eq. (4) is thus calculated in the following way: for each parameter (except T_S , γ , and N_0 : see below), and before each marginalization, typically 2×10^4 particles are propagated. The resulting histogram in time and energy is smeared out in energy with the AGASA energy resolution $\Delta E/E \sim 30\%$; this histogram is also convolved on the time axis with a top-hat of width T_S to represent a uniform emission of particles during the time T_S . With the same population of propagated nucleons, one can construct different histograms depending on γ and N_0 . The nucleons are indeed injected with an artificially flat spectrum between $10^{1.5} \text{ EeV}$ and 10^4 EeV , corresponding to $\gamma = 0$ to preserve satisfying statistics at high energies, and the counts on the detector are weighted in such a way as to reconstruct an injection spectrum with index γ . The likelihood is then marginalized over t_0 , and calculated for each T_S . New samples of nucleons are propagated to marginalize the likelihood over the different magnetic field realizations; finally, the last loop closes, the above process is repeated for each value of τ_{100} , and D . Due to the multi-dimensional nature of this likelihood, the size of the parameter space, notably the possible distances to the source, and the precision required (1 yr corresponds to $3 \times 10^{-7} \text{ Mpc}$), these simulations are very time consuming. They were carried out on IBM at the Max-Planck Institut für Physik, München (Germany), and on Alpha at the Institut d'Astrophysique de Paris, Paris (France).

We probe values for τ_{100} between $\simeq 0.1 \text{ yr}$ and 1000 yr . The lower bound is given by the size of our time bins whereas the upper bound is motivated by Faraday rotation limits on the extra-galactic magnetic field (e.g., Ref. [27]), which can be written as $(B_{\text{rms}}/10^{-9} \text{ G})(l_c/1 \text{ Mpc})^{1/2} \lesssim 1$, or,

$$\tau_{100} \lesssim 2.5 \times 10^3 \left(\frac{D}{30 \text{ Mpc}} \right)^2 \text{ yr} \quad (5)$$

[see Eq. (2)]. A comparable bound comes from the requirement that the relative deflection of the events in the AGASA pairs was smaller than the angular resolution $\simeq 1.6^\circ$ [41].

As to the source activity time scale, we choose the range $0.01 \text{ yr} \leq T_S \leq 10^3 \text{ yr}$ which, together with $1 \leq$

$N_0 \leq 4000$, brackets the range where the likelihood function should peak, given a couple of events observed within 5 yr. We note that, as long as the total UHECR output of the source, characterized by $\mathcal{E}(> 10^{1.5}\text{EeV})$ or N_0 [see Eq. (3)], is unconstrained, the likelihood analysis cannot distinguish between different values for T_S and τ_{100} that are considerably larger than the integration time T_{obs} of the experiment. In this limit, the likelihood becomes degenerate and only depends on the ratio(s) N_0/T_S or N_0/τ_{100} , i.e., the actual fluxes as seen by the experiment. Strictly speaking, it would be more appropriate to introduce the deviation around τ_{100} in the latter ratio, instead of τ_{100} ; however, at a given energy, this deviation is always a finite fraction of τ_{100} whose size only depends on whether the deflection is large or small compared to the coherence length [26].

It is interesting to note that pairs 2 and 3 do not show arrival energies inversely correlated to their arrival times, as would be expected from Eq. (2), whereas pair 1 does. As mentioned in the introduction, this flip around of time and energy for these pairs could be explained by the finite width of the $\tau_E - E$ correlation, i.e., the combination of the scatter due to the stochastic nature of the magnetic field, and of the finite instrumental energy resolution. Nevertheless, this could still be insufficient for pairs 2 and 3; in this case, these pairs would tend to favor a continuous source, where a flip around can simply result from different emission times. We will observe each of these tendencies in Sec.4.

Finally, we restrict ourselves to the limit of small deflections, $D\theta_E \ll l_c$. In effect, since the three pairs observed by AGASA imply $\theta_E \lesssim 2.5^\circ \simeq 0.044$, the limit $D\theta_E \gg l_c$ would require $D/l_c \gg 25$ and thus a rather large lattice in our code. Moreover, since the AGASA pairs also imply $D \lesssim 50$ Mpc, due to pion production, this case would only be realized if $l_c \ll 2$ Mpc. This is not likely in the case of an extra-galactic magnetic field, due to possible damping of the field on small scales $\lesssim 1$ Mpc [33]. If the deflection of UHECRs is dominated by the halo magnetic field, the distance to the source in Eq. (2) has to be replaced by the linear extension of the magnetic halo l_H (if the source lies outside of this halo); in this case, the limit $D\theta_E \gg l_c$, would necessitate $l_c \ll 4$ kpc if $l_H \lesssim 100$ kpc.

III. RESULTS

Since the likelihood function depends on so many variables we will present several one- and two-dimensional cuts through the parameter space. Because the values of most of the parameters are basically unconstrained it is also convenient to marginalize over one or several of the variables. In order to do so, one has to choose a suitable Bayesian prior. We will always assume a Jeffrey prior, i.e., uniform distributions in the logarithm of the variables τ_{100} , T_S , and N_0 . This choice is motivated by

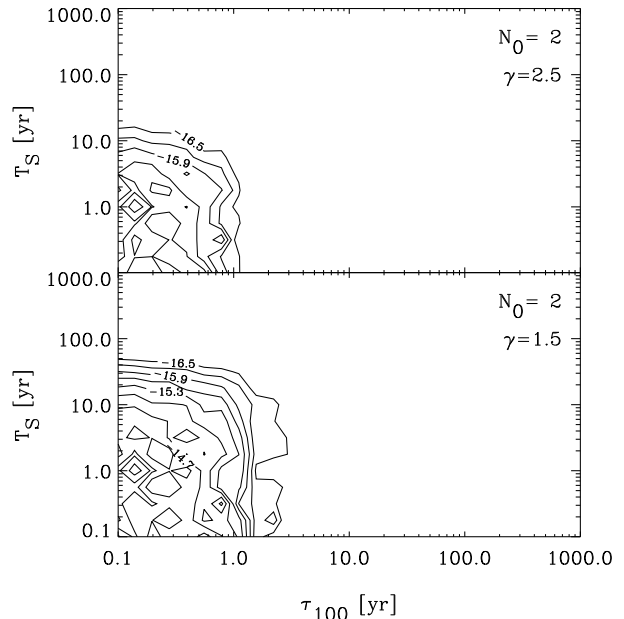


FIG. 2. Contour plots of the log-likelihood $\log_{10} \mathcal{L}$ in the $\tau_{100} - T_S$ plane for pair 1. The corresponding parameters are $D = 30$ Mpc, $n_B = 0$, $l_c = 1$ Mpc; N_0 and γ as indicated. The bottom panel corresponds to the maximum of the likelihood.

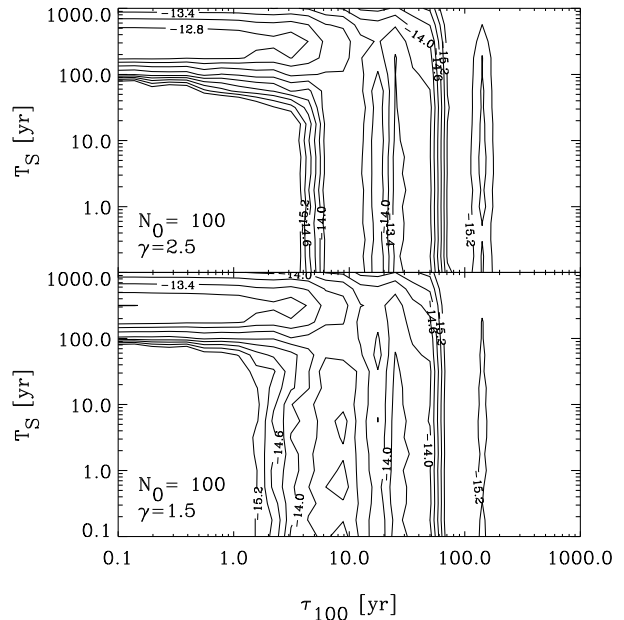


FIG. 3. Same as Fig. 2, but for pair 2.

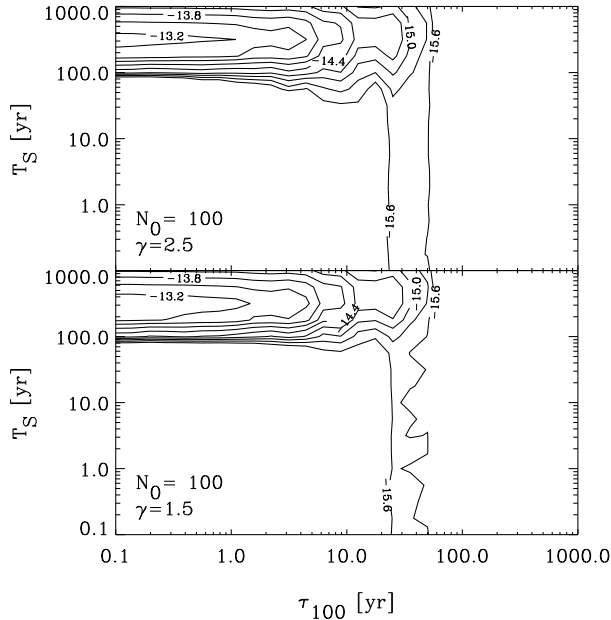


FIG. 4. Same as Fig. 2, but for pair 3.

the “scale invariance” of the problem, namely the fact that the time delay depends on powers of the magnetic field strength and coherence length, which are totally unknown, as well as the fact that the emission time scale and energy output are unknown within many orders of magnitude. We will thus consider the following types of representations in all of which $D = 30\text{Mpc}$, $n_B = 0$, and $l_c = 1\text{Mpc}$ take specific constant values, for illustration:

1. For a given N_0 , contour plots of the likelihood $\log_{10}(\mathcal{L})$ are shown in the $\tau_{100}-T_S$ plane, for two extreme values of the power-law index of the injection spectrum, $\gamma = 1.5$, and $\gamma = 2.5$, see Figs. (2–4).
2. The likelihood $\mathcal{L}(N_0)$, as marginalized over T_S and τ_{100} , is shown in Fig. (5). Via Eq. (3), this determines the most likely value for the total energy output $\mathcal{E}(> 10\text{EeV})$ of the source.
3. The likelihood $\mathcal{L}(\tau_{100}, T_S \ll 0.1\text{yr})$ marginalized over N_0 is shown in Fig. (6). This particular marginalization assumes a bursting source, and thus allows to determine the most probable corresponding time delay. Notably, the model of origin of UHECRs in cosmological γ -ray bursts requires $\tau_{100} > 50\text{yr}$ [17,18].
4. The likelihood $\mathcal{L}(T_S)$, as marginalized over τ_{100} and N_0 , is shown in Fig. (7). This marginalization allows to test the respective significance of a bursting or a continuous source.

From the figures shown here it is obvious that there are too many parameters for the current number of observations available. However, the following trends are discernible:

- In the limit of a high number of particles, the typical time dispersion, i.e., either T_S or the deviation around τ_{100} , scales like N_0 , so that the particles are spread out in time on the detector; i.e., so that the observed flux matches the injected flux. The likelihood thus becomes degenerate, and depends only on the ratios N_0/T_S , and/or N_0/τ_{100} , as argued in Sec.2. This degeneracy arises whenever $T_S \gg T_{\text{obs}}$, or the dispersion of the time delay for the lower energy particle in the pair, is much larger than T_{obs} . This can be seen best in Figs. 6–8. In fact, pairs 2 and 3 (see Table I), in which the higher energy particle arrived later, favor, respectively marginally and clearly, a comparatively large T_S .
- Pair 1 marginally (i.e., within factors of a few in the likelihood) favors a hard injection spectrum, which is expected in order to produce a 200 EeV event. For $\tau_{100} \lesssim$ a few years it allows for a bursting source. This is mainly due to the fact that its energies and arrival times are inversely correlated, as expected from Eq. (2). The small magnitude of the corresponding $\tau_{100} \lesssim 1\text{yr}$ results from the small difference in arrival times as compared to the significant difference in arrival energies (see Fig. 6). The origin of this pair is therefore not straightforward to account for.
- Pair 2 is insensitive to γ , since the energies of the particles are very close to each other. It allows for a burst with a large time delay, although the arrival times and energies are not inversely correlated. As argued previously, the flip around of the energies can be explained by the finite instrumental energy resolution. In our case, the instrumental resolution $\Delta E/E \sim 30\%$ dominates over the intrinsic scatter [26] due to the scattering off the magnetic field. This width introduces a dispersion in time delay, $\Delta\tau_E/\tau_E = 2\Delta E/E$. Hence, provided the time delay is sufficiently large, there is significant scatter both in energies and arrival times. This explains the tendency of pair 2 to accept a large time delay. Although the marginalized likelihood $\mathcal{L}(T_S)$ slightly favors $T_S \gtrsim 10\text{yr}$, this is not very significant and still consistent with a burst (see Fig. 7). This pair is thus consistent with an origin in cosmological γ -ray bursts.
- Pair 3, however, appears to be completely inconsistent with a burst for time delays $\tau_{100} \lesssim 100\text{yr}$. For larger time delays and correspondingly high total expected number of particles N_0 , this pair could be consistent with a burst. However, such high time delays might in turn be inconsistent with the Faraday rotation limit, as given by Eq. (5). Furthermore, the likelihood is suppressed by roughly a factor of 100 for such a scenario (see Figs. 4 and 7). Overall, and within the parameter space probed here, this pair seems to favor an origin in a

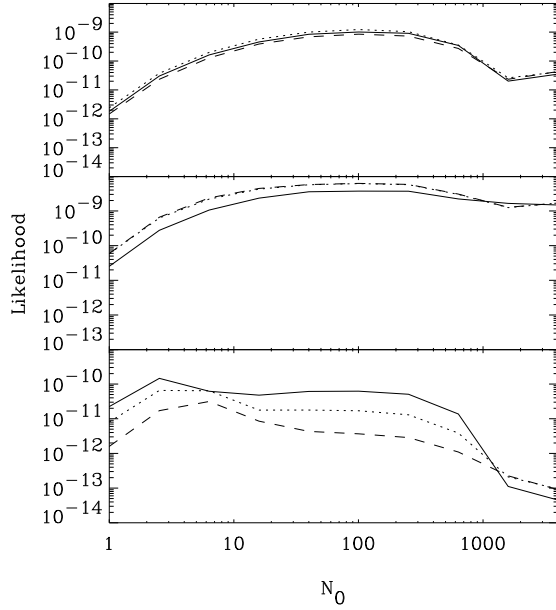


FIG. 5. Likelihood marginalized with respect to τ_{100} and T_S , plotted *vs* N_0 , for pair 1 (bottom panel), pair 2 (middle panel), and pair 3 (top panel). The solid lines correspond to $\gamma = 1.5$, the dotted lines to $\gamma = 2.0$, and the dashed lines to $\gamma = 2.5$. The parameters D , n_B , and l_c are the same as in Figs. 2–4. The decrease for $N_0 > 500$ for pair 1 and 3 is explained by the fact that in this range one would expect more than 2 events per 5 yr since $T_S \leq 10^3$ yr in our simulations. Due to the lower energies this can be compensated by a large time delay in case of pair 2.

continuous source with a high total energy output, corresponding to $N_0 \gtrsim 100$.

- In all cases the likelihood function tends to peak in the range where $\tau_{100} \lesssim 10$ yr. This is not significant for pair 2, which seems consistent with a burst and a comparatively long time delay; for pairs 1 and 3, however, the likelihood peak is at least a factor 10 higher than any value in the domain $\tau_{100} > 10$ yr. Using Eq. (2), this can be transformed into the tentative limit

$$B_{\text{rms}} \lesssim 6 \times 10^{-11} \left(\frac{l_c}{1 \text{ Mpc}} \right)^{-1/2} \left(\frac{D}{30 \text{ Mpc}} \right)^{-1} \text{ G}. \quad (6)$$

If confirmed, or possibly even improved by future data, this constraint would be more stringent than existing limits [27] by more than an order of magnitude.

We also performed runs for $D = 10$ Mpc and $D = 60$ Mpc, as well as for $n_B = 4$ and for $l_c = 10$ Mpc. For corresponding values of the parameters in Eq. (4), the likelihood does not significantly depend on n_B and l_c .

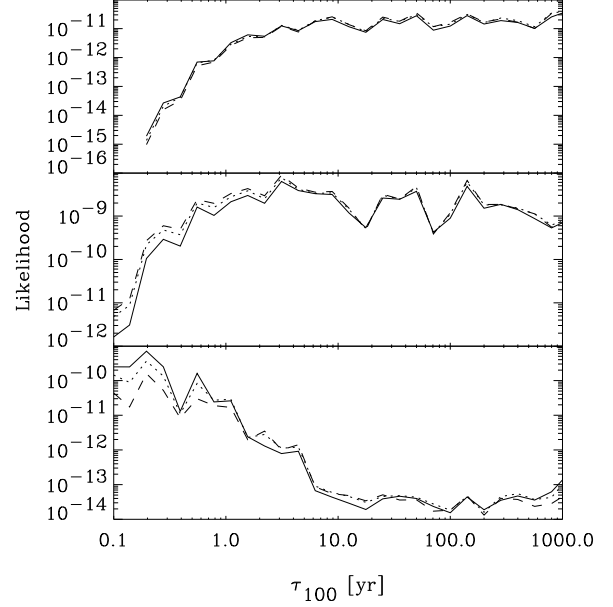


FIG. 6. Likelihood marginalized with respect to N_0 , assuming a bursting source, $T_S \ll 1$ yr, plotted *vs* τ_{100} , for pair 1 (bottom panel), pair 2 (middle panel), and pair 3 (top panel). The solid lines correspond to $\gamma = 1.5$, the dotted lines to $\gamma = 2.0$, and the dashed lines to $\gamma = 2.5$. The parameters D , n_B , and l_c are the same as in Figs. 2–4. This particular marginalization allows to estimate the most probable time delay, assuming a bursting source.

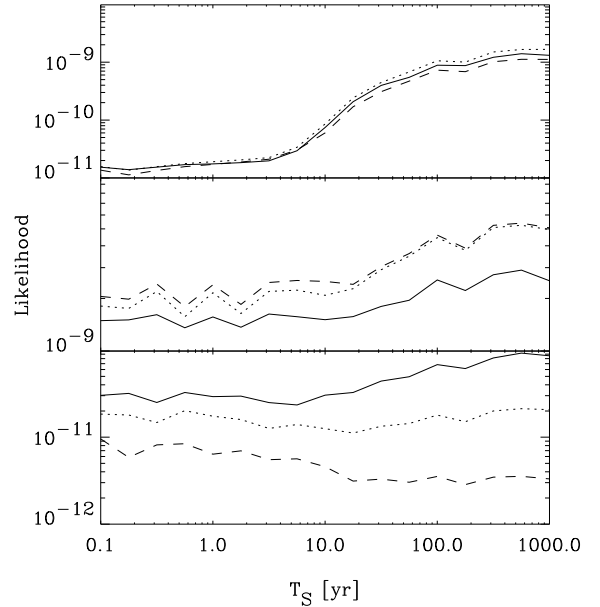


FIG. 7. Likelihood marginalized with respect to τ_{100} and N_0 , plotted *vs* T_S , for pair 1 (bottom panel), pair 2 (middle panel), and pair 3 (top panel). The solid lines correspond to $\gamma = 1.5$, the dotted lines to $\gamma = 2.0$, and the dashed lines to $\gamma = 2.5$. The parameters D , n_B , and l_c are the same as in Figs. 2–4.

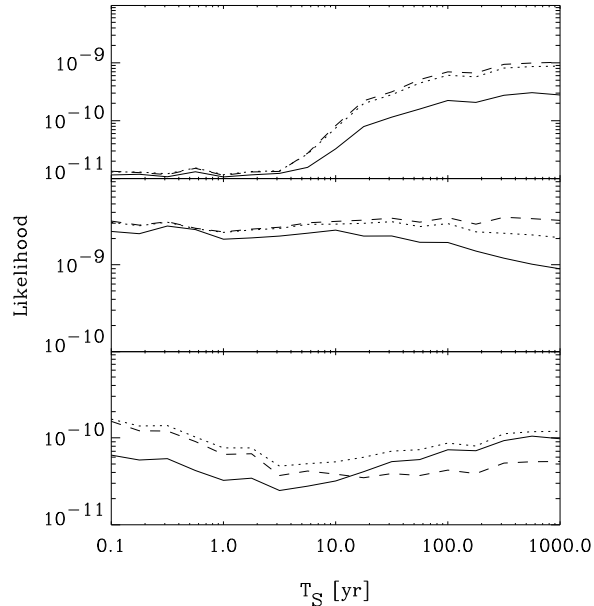


FIG. 8. Same as Fig. 7, but for a source at $D = 100$ kpc and a galactic halo field with $n_B = 4$, and $l_c = 30$ kpc, extending over 100 kpc.

For $D \lesssim 60$ Mpc the dependence on D is also insignificant, except possibly for pair 1 which favors $D \lesssim 30$ Mpc within a factor 3 – 4 in the likelihood.

Furthermore, we performed simulations for sources located within an extended galactic halo, in which case the time delay is dominated by the halo magnetic field. We chose a halo extension of 100 kpc with a coherence scale $l_c = 30$ kpc, $n_B = 4$, although the results again are not sensitive to these parameters. The maxima of the likelihood do not significantly differ from those obtained previously for a dominant extra-galactic magnetic field. The main difference between these two limits is the predominance of a soft spectrum $\gamma \simeq 2.0$ for pair 1, in the halo field case, even though this pair includes the 200 EeV event. This is demonstrated in Fig. 8 and can be attributed to the absence of frequent pion production. Furthermore, if D is now interpreted as the minimum of the source distance and the extension of the magnetized halo, Eq. (6) translates into the tentative constraint on the halo field

$$B_{\text{rms}} \lesssim 6 \times 10^{-7} \left(\frac{l_c}{1 \text{ kpc}} \right)^{-1/2} \left(\frac{D}{100 \text{ kpc}} \right)^{-1} \text{ G}. \quad (7)$$

Finally, we mention that the results presented in this section do not depend significantly on the lower boundary E_0 of the energy range over which we compute the likelihood function Eq. (4) as long as it is not much lower than the lowest event energy in the pairs, within the energy resolution. Lowering E_0 tends to make the γ -dependence of the likelihood function more significant, but neither a hard nor a soft injection spectrum can be

excluded for the sources of the three AGASA pairs.

IV. DISCUSSION AND CONCLUSIONS

Under our assumptions on the configuration of the LSMF, namely a power-law power spectrum down to some cutoff scale $l_c \gtrsim 1$ Mpc and $l_c \gtrsim 1$ kpc for time delays dominated by the extra-galactic or the galactic halo field, respectively, and within the limited range probed for the average time delay τ_{100} , our analysis suggests that all three AGASA pairs originated in different sources! Pair 1 would originate from a burst with a short time delay, $\tau_{100} \sim 1$ yr, i.e., a time delay inconsistent with that required in a cosmological GRB model. Pair 2 could originate from a burst, if the average time delay is sufficiently large, $\tau_{100} \gtrsim 50$ yr, as advocated in the cosmological GRB model, although it marginally favors a continuously emitting source with a high energy output. Finally, pair 3 cannot originate from a burst, unless the time delay is extremely large, and probably too large when compared to the Faraday rotation bound; it has to originate within a continuously emitting source, with $T_S \gtrsim 100$ yr, and $N_0 \gtrsim 100$, in agreement with conventional sources such as powerful radio-galaxies, for instance.

Let us now address the possibility of bursting topological defect sources. For example, certain classes of cosmic string loops might collapse and release all of their energy in form of UHECRs within about one light crossing time $T_S \ll 1$ yr [42], for symmetry breaking scales near the grand unified scale and typical total burst energies $\sim 10^{51}$ erg. For an LSMF $\gtrsim 10^{-11}$ G, events above $\simeq 80$ EeV are predicted to be most likely γ -rays, whereas around 50 EeV an approximately equal amount of protons is expected [43]. To take into account the likely γ -ray nature of the higher energy events in these models, a more accurate treatment should include propagation and deflection of electromagnetic cascades in the large-scale magnetic field. However, since for a given energy the amount by which an electromagnetic cascade particle and a nucleon is deflected and delayed is comparable, the topological defect scenario for the origin of UHECRs is not inconsistent with our above results, notably as far as pair 1 is concerned. In this respect, we note that the muon contents of the AGASA pairs air showers are not in contradiction with interpreting the higher energy event as a γ -ray [3]. The most efficient test of the topological defect scenario clearly resides in the chemical composition at energies $\gtrsim 80$ EeV, and improved data on UHECR composition could rule out this model in the future.

We do not wish to emphasize too strongly the above results, as quite a number of approximations had to be made, that restrict the range of parameter space available to us, and, furthermore, the statistics of the AGASA observations are limited. The main objective of the present work was, rather, to introduce the numerical code developed, and to give an example of what could be achieved

by future detectors. From our experience, it seems reasonable to say that one or several clusters of more than ~ 10 particles per source, would allow to pin down most of the parameters, notably: the magnetic field strength B_{rms} and coherence length l_c , the distance to the source D , the emission time scale T_S , and the time delay τ_{100} . Other parameters such as the differential energy index γ and the index of the power spectrum of magnetic inhomogeneities n_B (if any), are more difficult to grasp. In a separate paper, we present qualitative aspects of the angle-time-energy images of UHECR sources [39]; the qualitative features given there would allow to considerably restrain the size of the parameter space, and even give estimates of some of the above parameters. This would constitute a very useful first approach to a full likelihood evaluation.

In Ref. [44] it was shown that the γ -ray flux above 10^{19} eV contains information about the strength of the extra-galactic magnetic field. Here, we have shown that a likelihood analysis of clusters of charged UHECRs from a common extra-galactic source is also sensitive to the strength and the coherence scale in a range $10^{-12}\text{G} \lesssim B_{\text{rms}} \lesssim 10^{-9}\text{G}$, with $l_c \gtrsim 1\text{Mpc}$, and in addition to a possible galactic halo field in the range $10^{-8}\text{G} \lesssim B_{\text{rms}} \lesssim 10^{-6}\text{G}$, with $l_c \gtrsim 1\text{kpc}$. The deflection and delay of such UHECR clusters can thus be used as a new tool to probe the LSMF in a regime that is intermediate between field strengths accessible to conventional methods such as measuring the Faraday rotation of polarized light (see, e.g., Ref. [27]), and much weaker fields that could be detected by observing electromagnetic cascades in the TeV range [45,46]. The UHECR pairs observed by AGASA already indicate a trend towards comparatively small time delays, that can be translated into a tentative upper limit on the magnetic field strength, roughly an order of magnitude better than the Faraday rotation limit.

Future instruments in construction or in the proposal stage such as the Japanese Telescope Array [47], the High Resolution Fly's Eye [48], and the Pierre Auger Project [49] will have the potential to test whether there is significant clustering of UHECRs. The latter experiment, with an angular resolution of a fraction of 1° and an energy resolution of $\simeq 10\%$, should detect clusters of 20 – 50 events if the clustering observed by AGASA is real. With such statistics, it will be possible to answer the question on the nature of the sources of such UHECR clusters, and, in turn, to use these as “candles” to probe cosmic magnetic fields.

ACKNOWLEDGMENTS

We acknowledge P. Biermann, A. Dubey, C. Graziani, J. Quashnock, and D. Schramm for useful discussions. The Aspen Center for Physics is thanked for hospitality and support. We are grateful to Sangjin Lee for provid-

ing us with suitable pion and pair production tables from his thesis work. The Max-Planck Institut für Physik, München, Germany and the Institut d'Astrophysique de Paris, Paris, France, are thanked for providing CPU time. G.S. acknowledges financial support by the Deutsche Forschungs Gemeinschaft under grant SFB 375 and by the Max-Planck Institut für Physik. This work was supported, in part, by the DoE, NSF, and NASA at the University of Chicago, and by the DoE and by NASA through grant NAG 5-2788 at Fermilab.

-
- [1] D. J. Bird et al., *Astrophys. J.* **424**, 491 (1994).
 - [2] S. Yoshida et al., *Astropart. Phys.* **3**, 105 (1995).
 - [3] N. Hayashida et al., *Phys. Rev. Lett* **77**, 1000 (1996).
 - [4] K. Greisen, *Phys. Rev. Lett.* **16**, 748 (1966); G. T. Zatsepin and V. A. Kuzmin, *Pis'ma Zh. Eksp. Teor. Fiz.* **4**, 114 (1966) [*JETP. Lett.* **4**, 78 (1966)].
 - [5] M. Nagano et al., *Proc. 18th Texas Symposium*, eds. A. V. Olinto, J. Frieman, and D. N. Schramm, in press (World Scientific, Singapore, 1997).
 - [6] J. L. Puget, F. W. Stecker, and J. H. Bredekamp, *Astrophys. J.* **205**, 638 (1976).
 - [7] D. J. Bird et al., *Phys. Rev. Lett.* **71**, 3401 (1993).
 - [8] D. J. Bird et al., *Astrophys. J.* **441**, 144 (1995).
 - [9] N. Hayashida et al., *Phys. Rev. Lett.* **73**, 3491 (1994).
 - [10] G. Sigl, D. N. Schramm, and P. Bhattacharjee, *Astropart. Phys.* **2**, 401 (1994).
 - [11] J. W. Elbert and P. Sommers, *Astrophys. J.* **441**, 151 (1995).
 - [12] F. Halzen, R. A. Vazques, T. Stanev, and H. P. Vankov, *Astropart. Phys.* **3**, 151 (1995).
 - [13] A. M. Hillas, *Ann. Rev. Astron. Astrophys.* **22**, 425 (1984).
 - [14] G. Sigl and S. Lee, in *Proc. 24th International Cosmic Ray Conference (Rome) Vol. 3*, 356 (1995).
 - [15] R. Blandford and D. Eichler, *Phys. Rep.* **154**, 1 (1987).
 - [16] J. P. Rachen and P. L. Biermann, *Astron. Astrophys.* **272**, 161 (1993).
 - [17] E. Waxman, *Phys. Rev. Lett.* **75**, 386 (1995).
 - [18] E. Waxman, *Astrophys. J.* **452**, L1 (1995).
 - [19] M. Vietri, *Astrophys. J.* **453**, 883 (1995).
 - [20] M. Milgrom and V. Usov, *Astrophys. J.* **449**, L37 (1995).
 - [21] P. Mészáros, *Proc. 17th Texas Symposium (NY Acad. Sci. 1995)*.
 - [22] M. Vietri, *MNRAS* **278**, L1 (1996).
 - [23] P. Bhattacharjee, C. T. Hill, and D. N. Schramm, *Phys. Rev. Lett.* **69**, 567 (1992).
 - [24] C. T. Hill, *Nucl. Phys. B* **224**, 469 (1983).
 - [25] G. Sigl, *Space Sc. Rev.* **75**, 375 (1996).
 - [26] E. Waxman and J. Miralda-Escudé, *Astrophys. J.* **472**, L89 (1996).
 - [27] P. P. Kronberg, *Rep. Prog. Phys.* **57**, 325 (1994).
 - [28] S. Yoshida and M. Teshima, *Prog. Theor. Phys.* **89**, 833 (1993).
 - [29] R. J. Protheroe and P. A. Johnson, *Astropart. Phys.* **4**,

- 253 (1996).
- [30] S. Lee, report FERMILAB-Pub-96/066-A, e-print astro-ph/9604098, submitted to Phys. Rev. D.
 - [31] G. A. Medina Tanco, E. M. de Gouveia Dal Pino, and J. E. Horvath, e-print astro-ph/9610172, submitted to Astropart, Phys. (1996).
 - [32] M. J. Chodorowski, A. A. Zdziarski, and M. Sikora, *Astrophys. J.* **400**, 181 (1992).
 - [33] K. Jedamzik, V. Katalinić, and A. V. Olinto, e-print astro-ph/9606080 (unpublished).
 - [34] P. P. Kronberg and H. Lesch, *The Physics of Galactic Halos*, ed. Lesch et al. (Berlin: Akademie Verlag, 1996).
 - [35] T. Stanev et al., *Phys. Rev. Lett.* **75**, 3056 (1995).
 - [36] E. Waxman, K. B. Fisher, and T. Piran, *Astrophys. J.*, in press (1997).
 - [37] P. Biermann, H. Kang, and D. Ryu, Proc. of International Symposium on Extremely High Energy Cosmic Rays: Astrophysics and Future Observatories (Tokyo, 1996), 191.
 - [38] J. P. Rachen, Proc. 18th Texas Symposium, eds. A. V. Olinto, J. Frieman, and D. N. Schramm, in press (World Scientific, Singapore, 1997).
 - [39] M. Lemoine, G. Sigl, A. V. Olinto, and D.N. Schramm, submitted to *Astrophys. J.*
 - [40] W. H. Press, S. A. Teukolsky, W. T. Vetterling, and B. P. Flannery, *Numerical Recipes in Fortran*, 2nd. ed. (Cambridge: Cambridge University Press, 1992).
 - [41] J. W. Cronin, Proc. of International Symposium on Extremely High Energy Cosmic Rays: Astrophysics and Future Observatories (Tokyo, 1996), 2.
 - [42] P. Bhattacharjee, and N. C. Rana, *Phys. Lett. B* **246**, 365 (1990).
 - [43] G. Sigl, S. Lee, and P. Coppi, report FERMILAB-Pub-96/087-A, astro-ph/9604093, submitted to *Phys. Rev. Lett.*
 - [44] S. Lee, A. V. Olinto, and G. Sigl, *Astrophys. J.* **455**, L21 (1995).
 - [45] R. Plaga, *Nature* **374**, 430 (1995).
 - [46] E. Waxman, and P. Coppi, *Astrophys. J.* **464**, L75 (1996).
 - [47] M. Teshima et al. *Nucl. Phys. B (Proc. Suppl.)* **28B**, 169 (1992); M. Hayashida et al., Proc. of International Symposium on Extremely High Energy Cosmic Rays: Astrophysics and Future Observatories (Tokyo), 205 (1996).
 - [48] D. J. Bird et al., in Proc. 24th Cosmic-Ray Conf. (Rome), OG sessions, Vol. 2, 504 (1995); M. Al-Seady, M. et al., Proc. of International Symposium on Extremely High Energy Cosmic Rays: Astrophysics and Future Observatories (Tokyo), 191 (1996).
 - [49] J. W. Cronin, *Nucl. Phys. B (Proc. Suppl.)* **28B**, 213 (1992).